Journal of the Korean Electrochemical Society
Vol. 21, No. 1, 2018, 12-20
https://doi.org/10.5229/JKES.2018.21.1.12

pISSN 1229-1935
eISSN 2288-9000

Effects of Aluminum and Silicon as Additive Materials for the Zinc Anode in Zn-Air Batteries

Yong-Seok Lee and Kwang-Sun Ryu*

Department of Chemistry, University of Ulsan, Ulsan 680-749, Korea

(Received January 18, 2018 : Revised February 12, 2018 : Accepted February 13, 2018)

Abstract : To solve low cycle efficiency of the zinc anode in Zn-air batteries by corrosion, this study examined the effects of Al as a cathodic protection additive to Zn. The Al-mixed Zn anodes were produced by mixing Zn and Al powder (1, 2, and 3 wt. %). To compare the effects of the Al additive, Si was selected under the same conditions. The morphology and elemental composition of the additives in the Zn were characterized by scanning electron microscopy, energy dispersive X-ray spectroscopy, and inductively coupled plasma – mass spectrometry. The anti-corrosion effects of the Al and Si-mixed Zn anodes were examined by linear polarization. Cyclic voltammetry and charge-discharge tests were conducted to evaluate the electrochemical performance of the Al and Si-mixed Zn anodes. As a result, the Al-mixed Zn anodes showed highest corrosion resistance and cycling performance. Among these, the 2 wt.% Al-mixed Zn anodes exhibited best electrochemical performance.

Keywords : Zinc-air battery, Zinc anode, Aluminum, Silicon, Corrosion, Reversibility

1. Introduction

Zn-air batteries are promising candidates for secondary alkaline batteries as a replacement for lithium-ion batteries owing to their low cost and high specific energy density of 1086 Wh kg^{-1}.[1)] On the other hand, the batteries have not been commercialized as secondary batteries because of their poor reversibility and charge-discharge performance. One of the reasons for the low cycling performance the Zn anode contributes to the poor charge-discharge properties of Zn-air cell due to dendrite formation, corrosion reaction, and hydrogen evolution reaction (HER). In particular, zinc corrodes spontaneously due to the reaction between zinc and water, which leads to the HER. The side reaction consumes the alkaline electrolyte, resulting in a decrease in the efficiency of zinc and finally the poor cycle lifetime of Zn-air batteries.[1,2)]

In an attempt to solve this problem, many studies have been examined organic, inorganic, and surfactant additives or alloys with other metals.[3-9)] C. W. Lee *et al.* studied a Zn-Ni-In alloy anode due to the increasing hydrogen overpotential and reduction of the HER.[8)] C. J. Lan *et al.* produced a Zn-Al alloy anode. Because aluminum has a more negative redox potential than zinc, the OCV values of the Zn-Al anode have more negative potentials than the pure Zn electrode and the alloy anode showed high discharge capacities in the Zn-air cell system.[9)] In addition, aluminum is often used as a cathodic protection material suppressing zinc corrosion because it has a more negative oxidation potential than zinc.[10)] Therefore, aluminum reacts instead of zinc at the potential area of zinc corrosion and suppresses zinc corrosion and the HER.

The overall aim of this study was to suppress the corrosion reaction of zinc and improve the electrochemical performance of the zinc anode in Zn-air batteries using Al as an additive material. The Al-added Zn anode was prepared by mixing Al and Zn powders. In addition, for comparison with the effects of Al additives, Si was selected as the comparison target because it also has a more negative potential than zinc but lower than aluminum [11].

*E-mail: ryuks@ulsan.ac.kr

Therefore, Si may show a similar effect as an additive but the effect would less than that of aluminum due to the lower oxidation reactivity than aluminum. Also, for electrochemical analysis, a conventional three electrode system and Zn-air cell system were conducted. The anti-corrosion performance was measured by linear polarization. The cyclic voltammogram and charge-discharge tests were performed to evaluate the electrochemical performance.

2. Experimental

The Al and Si mixed Zn composites were prepared by grinding Zn powder (99%, Daejung chemical) and Al (99%, Daejung chemical) or Si powder (99.9%, Alfa Aesar) with 1, 2, and 3 wt. % of Zn powder. In the half-cell test, for the fabrication of zinc-based electrodes, the composite powders were mixed with 15 wt.% polytetrafluoroethylene (PTFE, 60 wt. % in D.I H_2O, Sigma-Aldrich).

In the full cell test, zinc gel anodes were fabricated. The anodes were composed of 65.6 wt. % 6M KOH (93%, Daejung chemical), 0.016 wt. % polyacrylic acid (PAA, Sigma-Aldrich) and 32.8 wt. % Zn powder with the Al and Si powders. For gelation, 6M KOH as the electrolyte was mixed with PAA as the gelling agent for 2h. After gelation, the powders were added and mixed with stirring for 10 min at room temperature. The contents of the Al and Si were 1, 2, and 3 wt. % of the zinc powders.

Surface morphology of the bare Zn, Al or Si added Zn powders were examined by scanning electron microscopy (SEM, Carl Zeiss Supra 40). Energy dispersive spectroscopy (EDS, Carl Zeiss Supra 40) and inductively coupled plasma - atomic emission spectrometry (ICP-AES, Thermo Electron iCAP6500) were performed to confirm the distribution and contents of the Al and Si powders in the Zn powders.

For the linear polarization and cyclic voltammetry test, the conventional three-electrode cell was adopted with a platinum wire as a counter electrode and a standard calomel electrode (SCE) as the reference electrode. The working electrode was pure zinc, Al-, and Si-added zinc electrodes, and 6 M KOH was used as the alkali electrolyte. Linear polarization was conducted to measure the hydrogen evolution reaction of the electrodes at -2.0 V for 30 min. To evaluate the electrochemical performance of the Al- and Si-added Zn electrode, cyclic voltammetry was conducted at a scan rate of 1mV/s from -2.3 V to -0.2 V. These measurements were performed using a computer controlled instrument (IVIUMSTAT, IVIUM Tech). The Zn-air cell was adapted to evaluate the charge-discharge test. Pure Zn and Al or Si added Zn gels were used as the anode and a commercialized air electrode (MEET ADE75) was adapted as the cathode. A microporous membrane (Celgard 3501 separator) was used as the separator. The air cells were charged and discharged at an applied current density of 65mA/g and a cut-off time of 30 min using a battery tester (Series 2000 battery tester, Marco) at room temperature.

3. Results and Discussion

3.1. Characterization of the Al- or Si-added Zn powder

Fig. 1 shows SEM images of (a) pure Zn, (b) pure Al, (c) pure Si particles, (d)-(f) 1, 2, and 3 wt. % Al-added Zn particles, and (g)-(i) 1, 2, and 3 wt. % Si-added Zn particles. The Al particles had a larger size than the Zn particles, whereas the Si particles had a smaller size than the Zn particles. As shown in Fig. (d)-(f), the Al particles appeared to be included in the Zn particles. The black color region in SEM images (d)-(f) are Al particles. The Si particles were not observed because of their small particle size.

SEM-EDS analysis was conducted to compare the dispersion of Al and Si particles. The mapping images in Fig. 2 (a)-(c) and (d)-(e) show the dispersion of Al and Si particles (Red color is Zn particles, green color is Al particles in (a)-(c), and blue color is Si particles). According to the increasing of Al and Si content, many added particles were observed in the images. Si particles were more dispersed than Al due to the difference in particle size. ICP-MS was conducted to determine the content of Al and Si accurately in the Zn powder matrix. The analyzed content of Al and Si is listed in Table 1. The content of Al in the 1, 2, and 3 wt. % Al-mixed Zn was determined to be

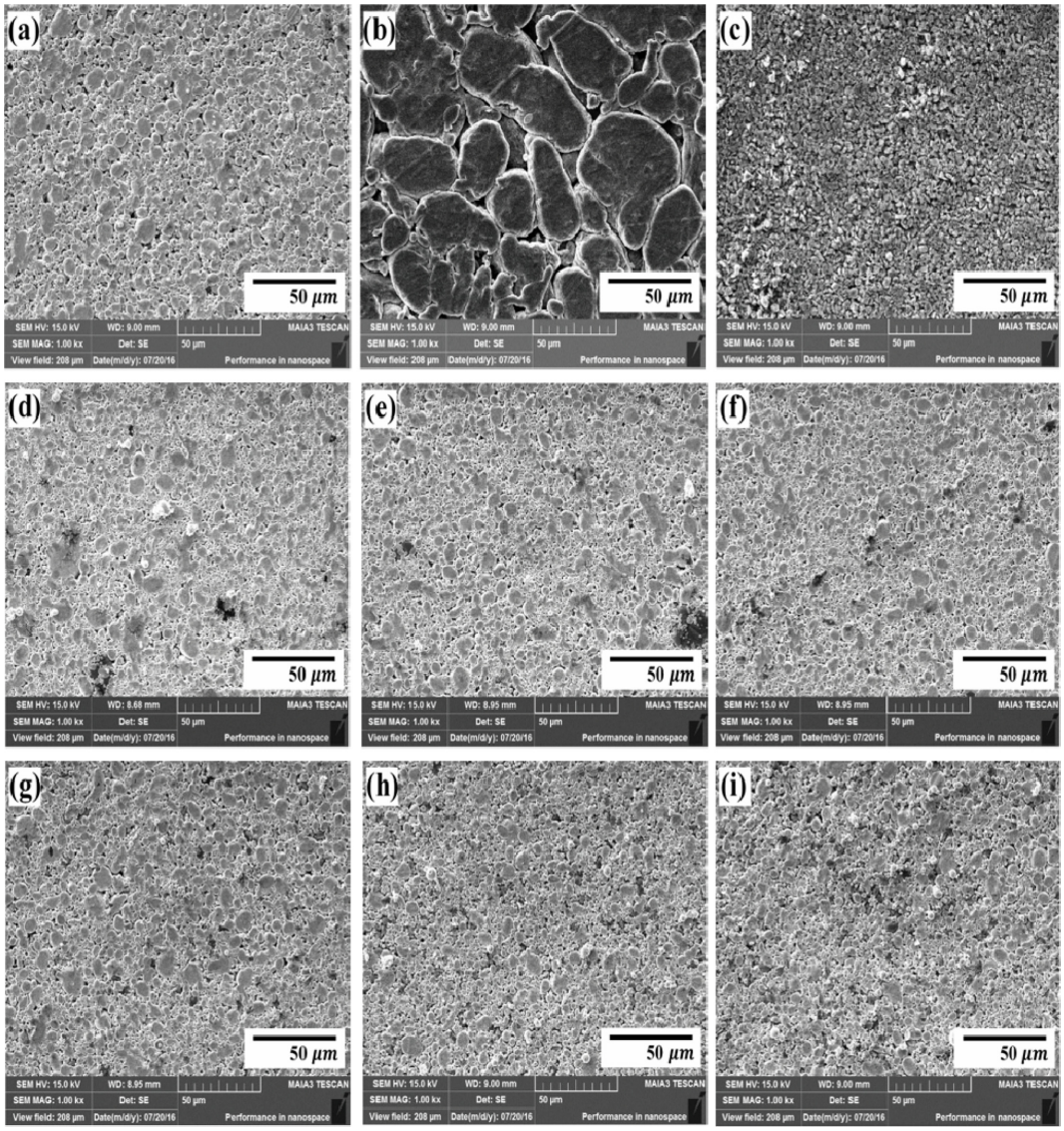

Fig. 1. FE-SEM images of (a) pure Zn particles, (b) pure Al particles, (c) Pure Si particles, (d)-(f) 1, 2, and 3 wt. % Al-mixed Zn particles, (g)-(i) 1, 2, and 3 wt. % Si-mixed Zn particles.

1.1, 2, and 3%, which is in good agreement with the expected value. In the case of Si, the content was 1.4, 2.3, and 3.0% respectively, which is slightly different from that observed with Al.

3.2. Electrochemical analysis

Linear polarization was performed to assess the effects of Al and Si as anti-corrosion additives. The Zn electrodes were tested at -2.0 V versus the SCE reference electrode. Fig. 3 (a) and (b) show linear polarization curves of the Al and Si-added Zn electrode with various contents. The corrosion current and corrosion resistance were calculated using the following equation [12].

$$R(\Omega) = \frac{\Delta I_{corr}}{E_{corr}} \quad (1)$$

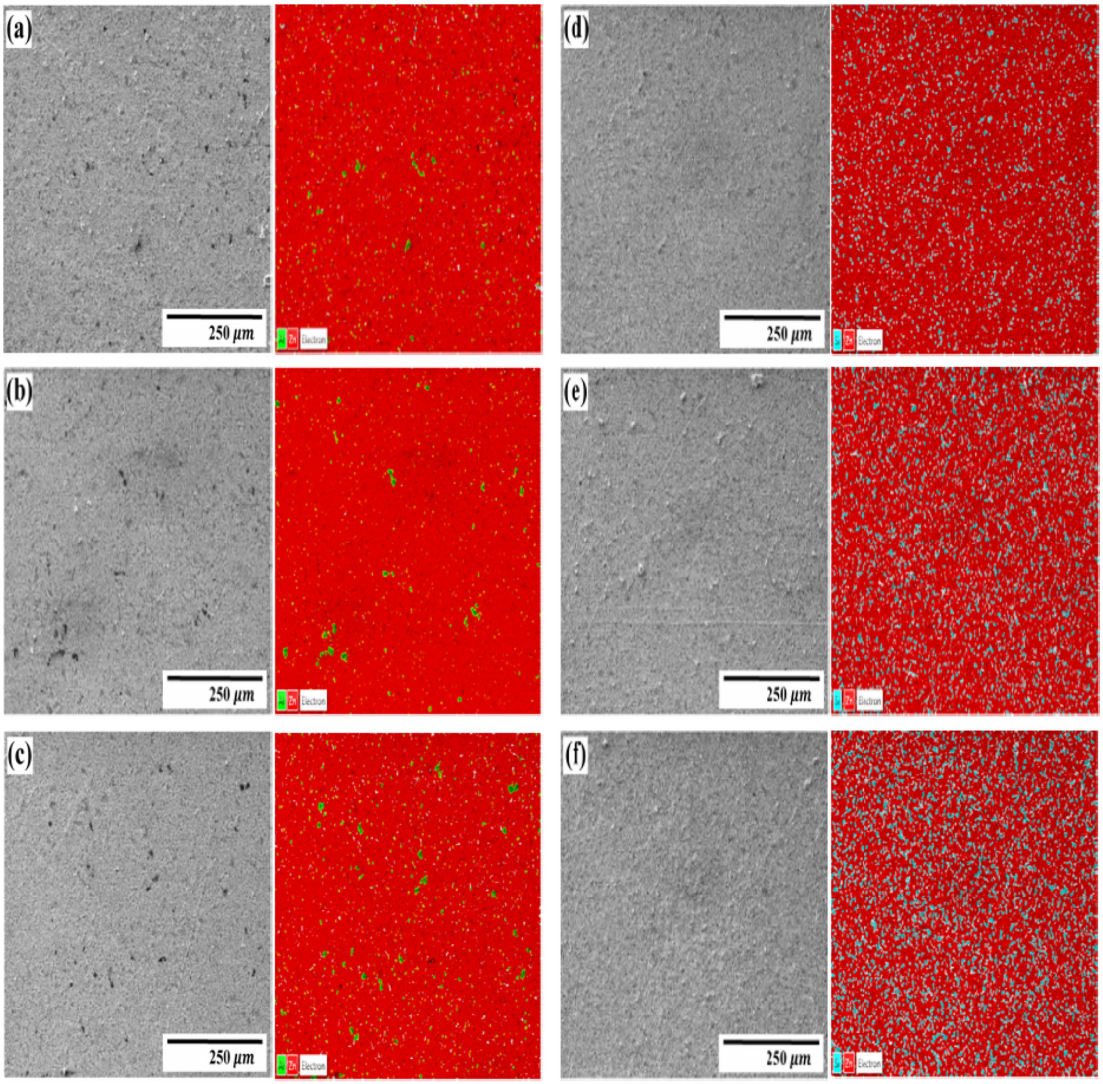

Fig. 2. EDS mapping images of (a)-(c) 1, 2, and 3 wt. % Al-mixed Zn particles, (d)-(f) 1, 2, and 3 wt. % Si mixed Zn particles.

Table 1. Al and Si content in Zn powders by ICP-AES analysis.

Sample	Al content (%)	Sample	Si content (%)
1 wt. % Al	1.1	1 wt. % Si	1.4
2 wt. % Al	2.0	2 wt. % Si	2.3
3 wt. % Al	3.0	3 wt. % Si	3.0

where R is the corrosion resistance, and ΔI_{corr} and E_{corr} are the corrosion current and corrosion potential (-2.0 V) applied to this test, respectively. We have observed a small bump at the initial state of the curve of Al-mixed Zn electrodes. This may be due to the high instantaneous current of the electrodes by higher

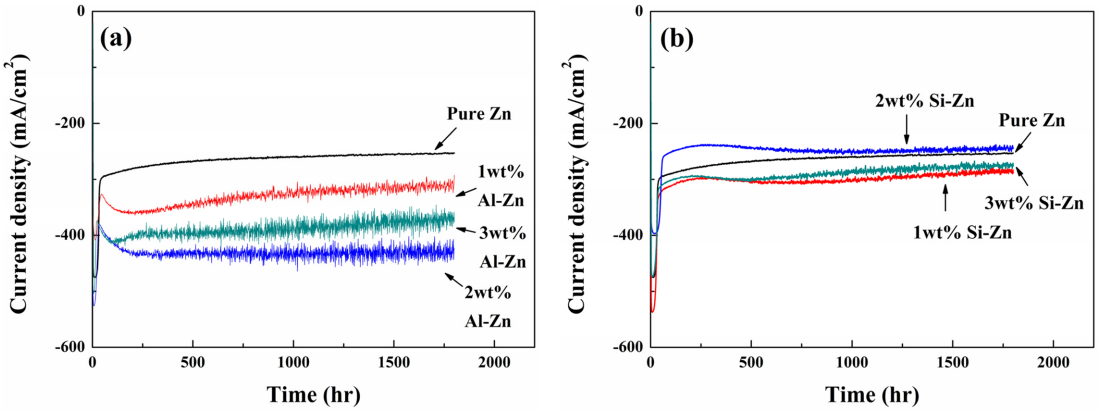

Fig. 3. Linear polarization curves of (a) pure Zn and Al-mixed Zn anodes and (b) pure Zn and Si-mixed Zn anodes.

Table 2. Corrosion resistance from the linear polarization curve.

	Initial current (mA/cm^2)	Final current (mA/cm^2)	ΔI_{corr} (mA/cm^2)	R_p (Ω)
Zn bare	475	253	222	9.01
Al 1 wt. %	408	292	115	17.4
Al 2 wt. %	526	423	103	19.4
Al 3 wt. %	504	376	128	15.6
Si 1 wt. %	537	288	249	8.03
Si 2 wt. %	397	244	153	13.1
Si 3 wt. %	473	276	197	10.2

electronical conductivity than Zn and Si.

Table 2 lists the calculated results. At all Al and Si contents, the corrosion resistance was reduced except for 1 wt. % Si. This means that Al and Si react with the alkaline electrolyte (H_2O) at the potential area of the corrosion reaction instead of Zn. Among them, the Al-added Zn electrode showed lower corrosion resistance than the Si-added electrode. This may be because the oxidation potential of Al is closer to the HER potential of Zn than Si. In terms of content, the 2 wt. % Al- and Si-added Zn electrodes exhibited the highest corrosion resistance.

3.3. Cyclic voltammetry

Cyclic voltammetry was conducted to evaluate the electrochemical properties of the Al- and Si-added Zn electrodes from -2.3 V to -0.2 V versus the SCE in 6M KOH at a scan rate 1mV/s. Fig. 4 shows the cyclic voltammograms of the (a) pure zinc and (b)-(d) Al-mixed Zn anode with various contents. To evaluate the electrochemical properties, the polarization between the anodic and cathodic current peak was calculated first. The peak separation, meaning polarization, was taken as an estimate of the reversibility of the oxidation and reduction reactions.[13,14] Table 3 lists the calculated polarization. Compared to the pure Zn and Al-mixed Zn anodes, the polarization decreased except for the 1 wt. % Al-mixed Zn anode. In particular, the 3 wt. % Al-mixed Zn anode showed the smallest peak separation (691 mV). Secondly, the anodic and cathodic peak areas were considered to estimate the cycling efficiency. Because the peak area in the cyclic voltammograms means the charge and capacities, the peak area of the anodic and cathodic indicates the efficiency of the oxidation and reduction reaction.[3] The 3 wt. % Al-mixed Zn anode exhibited a larger oxidation area than the pure Zn anode at the 1st anodic reaction. On the other hand,

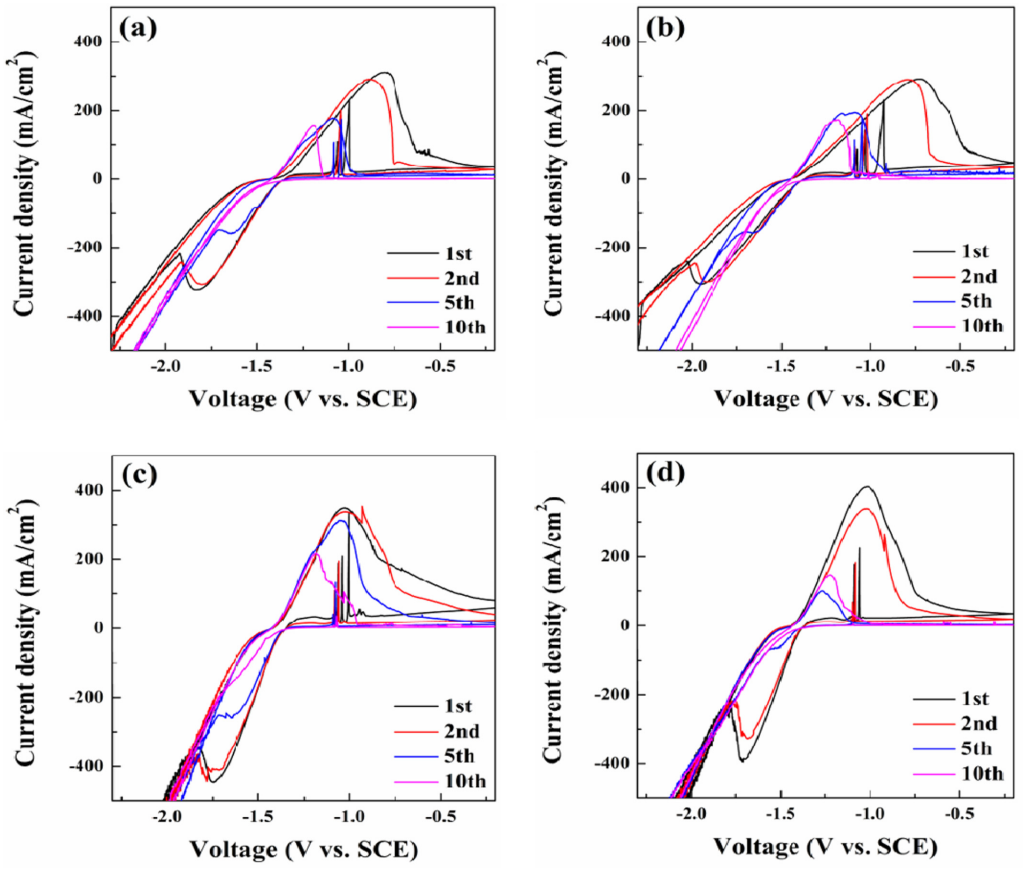

Fig. 4. Cyclic voltammograms of (b) pure Zn anode, (b) 1 wt. %, (c) 2 wt. %, and (d) 3 wt. % Al-mixed Zn anodes.

Table 3. Polarization between anodic and cathodic reaction.

	E_{anodic} (mV)	$E_{cathodic}$ (mV)	$\Delta E_{a,c}$ (mV)
Zn bare	-813	-1829	945
Al 1 wt. %	-733	-1942	1209
Al 2 wt. %	-1046	-1746	700
Al 3 wt. %	-1023	-1714	691
Si 1 wt. %	-892	-1821	929
Si 2 wt. %	-934	-1712	778
Si 3 wt. %	-1023	-1511	448

the lowest oxidation and reduction peak area was obtained from the 5th ~ 10th cycle. This means that the reversibility of the 3 wt. % Al mixed Zn anode is lower than that of the pure Zn anode. The Al reacts with H_2O to produce H_2 bubbles that hinder the diffusion of Zn^{2+} and OH^- ions. In contrast, the 1 wt. % and 2 wt. % Al mixed Zn anodes showed higher oxidation and reduction peak areas from the 1st ~ 10th cycle. Among them, the 2 wt. % Al-mixed Zn anode exhibited a reduction peak area at the 10th cycle. This explains why the 2 wt. % Al-mixed Zn anode has the highest cycling efficiency. According to the polarization and cycling efficiency tests, the 2 wt. % Al-mixed anode showed the high-

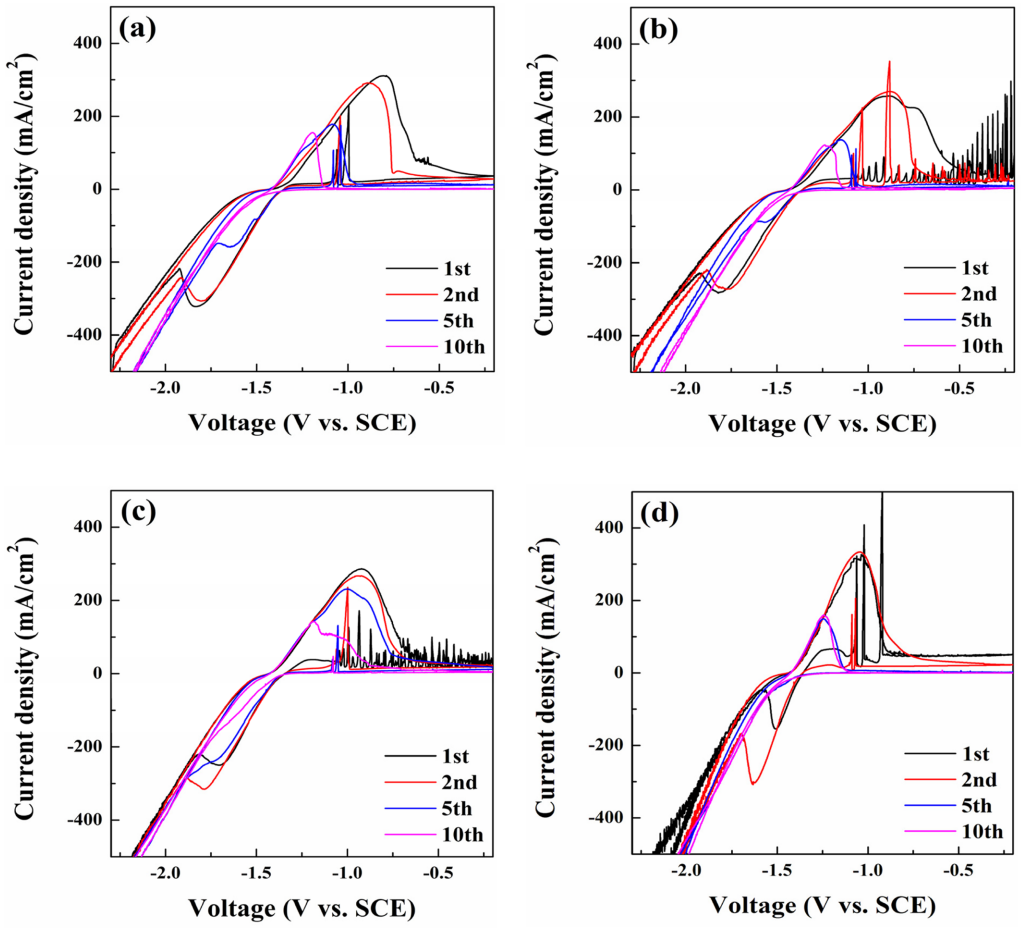

Fig. 5. Cyclic voltammograms of (b) pure Zn anode, (b) 1 wt. %, (c) 2 wt. %, and (d) 3 wt. % Si-mixed Zn anodes.

est reversibility.

Fig. 5 shows cyclic voltammograms of the (a) pure zinc and (b)-(d) Si-mixed Zn anode with various contents. The Si-mixed Zn anode showed similar peak separation to the Al-mixed Zn anodes. On the other hand, the oxidation and reduction peak areas were not increased. In addition, the reduction peak area of the 3 wt. % Si-mixed Zn anode was not observed. This means that the cycling efficiency of the anode was not improved. This may be because the oxidation potential of Al is closer to the HER potential of Zn than Si. Therefore, the Si additives have a lesser effect than the Al additive. When the oxidation and reduction peak areas from the 1st to 10th cycles were examined, the 2 wt. % Si-mixed anode showed improved cycling efficiency compared to the pure Zn anode.

3.4. Cycling performance

A charge-discharge Zn-air cell test was conducted to evaluate the cycling durability of the Al- and Si-mixed Zn anode at a current density of 65 mA/g and a cut-off time of 30 min. Fig. 6 shows the charge-discharge curves of (a) bare Zn, (b)-(e) Al-mixed Zn anode with various contents. The end condition of the cycling tests was set when the voltage of the air cells moved off the working voltage area of the Zn-air cell (0 V to 2.3 V). The pure Zn electrode was examined for 15 hours while the Al-mixed Zn electrodes were examined for 16

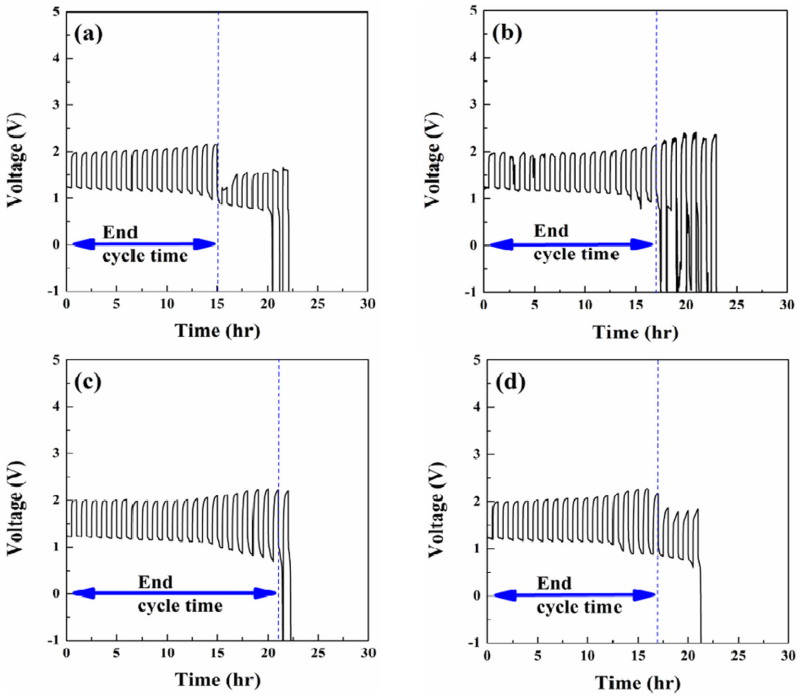

Fig. 6. Charge-discharge tests (a) pure Zn anode, (b) 1 wt. %, (c) 2 wt. %, and (d) 3 wt. % Al-mixed Zn anodes.

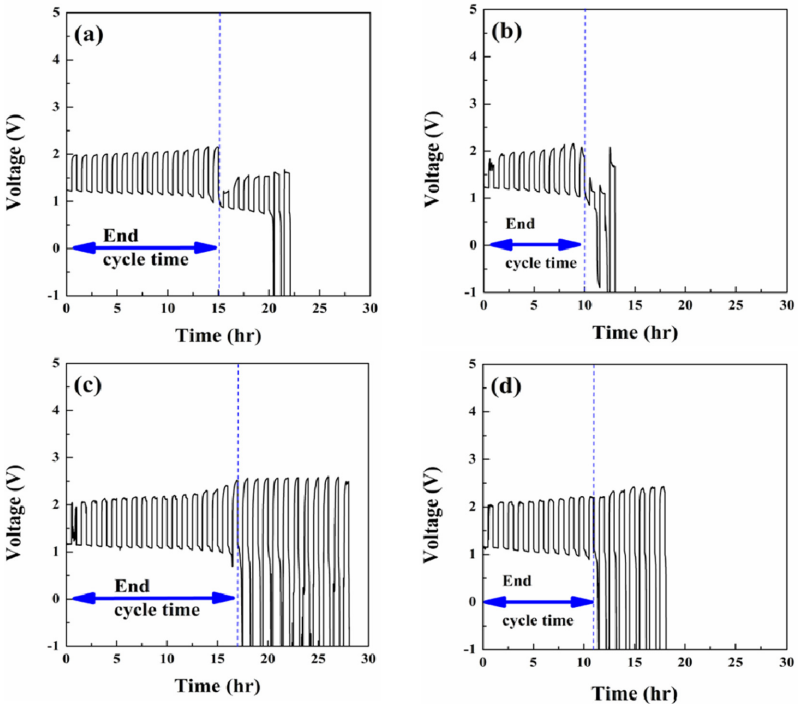

Fig. 7. Charge-discharge tests (a) pure Zn anode, (b) 1 wt. %, (c) 2 wt. %, and (d) 3 wt. % Si-mixed Zn anode.

hours (1 wt. %), 21 hours (2 wt. %), and 17 hours (3 wt. %). This corresponds to the results of linear polarization and cyclic voltammograms. Because Al reacts with H_2O at the potential area of the corrosion reaction of Zn, the HER by Zn is suppressed and the efficiency of the Zn anode is increased. As a result, the reversibility and cycling durability of the Zn anodes were improved. Unlike the Al-mixed Zn anodes, the Si-mixed Zn anodes showed a lower reducibility and cycling durability than the pure Zn electrode except for the 2 wt. % Si-mixed anode (Fig. 7). Only the anode mixed with 2 wt. % Si was examined by 16 times (vs. 15 times of pure Zn). On the other hand, the performance of 2 wt. % Si was different from that of pure Zn. In addition, the 1 and 3 wt. % Si-mixed anodes showed a poor cycle lifetime. It may be related to a side reaction, which was observed as sharp peaks in the cyclic voltammogram at 1 cycle.

4. Conclusion

Al or Si was adapted as anti-corrosion additives for the Zn electrode in Zn-air batteries. The materials were mixed with Zn (1, 2, and 3 wt. %). SEM confirmed the morphologies of the Zn, Al, and Si powder. EDS mapping and ICP-AES were conducted to examine the dispersion of Al or Si in the Zn matrix. Linear polarization showed that the Al or Si-mixed Zn anodes had higher corrosion resistance than the pure Zn anode. Cyclic voltammetry and the charge-discharge cyclic tests showed that the reversibility and efficiency of the Zn anode were improved in the systems of the half cell and Zn-air full cell. A comparison of Al and Si revealed the Al-mixed Zn electrodes to have a better anti-corrosion effect and electrochemical performance than the Si-mixed the electrodes due to more negative oxidation potential of Al than that of Si. Among the Al-mixed electrodes, the 2 wt. % Al-mixed electrodes showed the longest cycle lifetimes.

Acknowledgement

This study was supported by a National Research Foundation of Korea (NRF) grant funded by the Korean Government (MEST) (NO. 2012-M1A2A2).

References

1. Y. Li, H. Dai. *Chem Soc Rev.*, **43**, 5257-5275 (2014).
2. G. Toussaint, P. Stevens, L. Akrour, R. Rouget, F. Fourgeot. *J. Electrochem. Soc.*, **28**, 25-34 (2010).
3. J. Vatsalarani, S. Geetha, D. C. Trivedi, P. C. Warrier. *J. Power Sources*, **158**, 1484-1489 (2006).
4. Y. D. Cho, G. T. K. Fey. *J. Power Sources*, **184**, 610-616 (2008).
5. J. Huang, Z. Yang, B. Yang, R. Wang, T. Wang. *J. Power Sources*, **271**, 143-151 (2014).
6. C. W. Lee, K. Sathiyanarayanan, S. W. Eom, H. S. Kim, M. S. Yun. *J. Power Sources*, **160**, 1436-1441 (2006).
7. J. Dobryszycki, S. Biallozor. *Corrosion Science*, **43**, 1309-1319 (2001).
8. C. W. Lee, K. Sathiyanarayanan, S. W. Eom, H. S. Kim, M. S. Yun. *J. Power Sources*, **159**, 1474-1477 (2006).
9. C. J. Lan, T. S. Chin, P. H. Lin, T. P. Perng. *J. New Mat. Electrochem. Systems*, **9**, 27-32 (2006).
10. T. Kaewmaneekul, G. Lothongkum. *Corrosion Science*, **66**, 67-77 (2013).
11. L. David R., ed. CRC Handbook of Chemistry and Physics. 87th ed. Boca Raton (FL): *CRC Press*, p. 2608. (2006)
12. Y. Ein-Eli, M. Auinat, D. Starosvetsky. *J. Power sources*, **114**, 330-337 (2003).
13. L. Bing, Y. Huatang, Z. Yunshi, Z. Zuoxiang, S. Deying, *J. Power Sources*, **79**, 277-280 (1999).
14. Dennis A. Corrigan, Richard M. Bendert, *J. Electrochem. Soc.*, **136**, 723-727 (1989).